Van de Graaff: Lifetime of ^{11}C

Author: James Dragan

Affiliation: Richard Lefferts

Lab Partner: Stefan Evans

Physics Department, Stony Brook University, Stony Brook, NY 11794.

(Dated: November 4, 2013)

We present the procedure to create a ^{11}C sample by bombarding ^{11}B with a high energy (HE) proton beam and then measure its half-life. The proton beam is accelerated to energies near 6 MeV using a Tandem Van de Graaff. The procedure to tune the proton beam to target is also discussed. For data collection, we show the optimization of data collection parameters used in measuring the coincidence count rate of .511 MeV gamma ray detection from a 1 μCi ^{22}Na source. Using these settings we measured the half-life of ^{11}C to be $t_{1/2} = 20.31^{+0.089}_{-0.068}$ min.

1.   MOTIVATION

The purpose of this lab is to measure the lifetime of $^{11}_6$C. Unfortunately this isotope is not naturally occurring, there is no primordial $^{11}_6$C leftover nor is there any local cosmic source. In addition any reactor through neutron capture or fission creates neutron rich elements, while we want neutron poor. Therefore we turn towards an accelerator to produce the isotope we need. Because Stony Brook University has a Tandem Van de Graaff we use this. Using this apparatus we are able to create a $^{11}_6$C source and measure its lifetime.

2.   PROCEDURE

2.1.   Ion Source

We use a General Ionex 860A Inverted Sputter negative ion source. Here a Cesium (Cs) boiler is set to a temperature of 139.43°C so that it boils and travels up toward a Tantalum (Ta) ionizer. The Ta coil is heated by an applied current to about 1200°C. The Cs condenses onto the Ta coil, then boils off but becomes ionized as it leaves an electron due to its lower ionization potential[1]. This Cs$^+$ ion is accelerated towards a cathode rod with a Hydrogen doped Titanium (TiH$_x$) sample by a potential difference of - 3.94 kV. The Cs$^+$ penetrates into the TiH$_x$ several atomic layers deep. Upon collision Hydride (H$^-$) among other negative ions is ejected from the TiH$_x$ and is attracted away from the cathode by a -14.96V extraction potential whose ground is located past the Tantalum ionizer. The sputtering, or splash of materials, is naturally diverging based upon the kinematics of the collision between the Cs$^+$ ion and the TiH$_x$ sample and as a result we need to focus this negative ion beam.

2.2.   Einzel Lens

This lens is completely analogous to a typical optical lens, except it uses a variable electric field to focus, instead of shape and indices of refraction. Here we have two grounded cylinders separated by a Nickel mesh which has a 4.46 kV applied voltage. A ion traveling directly along the axis of propagation, z-axis, will feel no force (understood by drawing the field lines). In contrast an ion traveling with an off axis component of velocity will be accelerated from a 'slow' velocity to some faster velocity based upon the potential difference, and based upon the field lines it is accelerated towards the center. When it reaches the nickel mesh the beam undergoes a defocusing

but because it has a higher speed the divergence is not as stark and its convergence towards the center when it was focused. Simply put, the rate of focusing when the beam is slow is stronger than the defocusing when the beam is traveling at a faster velocity. This principle is used several more times throughout this experiment to continually focus the beam.

2.3. Mass Selector

We apply a current producing a magnetic field of strength chosen to allow the ion of our interest to pass, while the other ions, because of their mass, will deflect and hit the walls. Initially the selection is for oxygen because of known contamination to the beam, not large enough to concern us. We will maximize the beam current for oxygen then to select for a mass of 0.97 a.u. which is just below the atomic weight of H^-. Due to hysteresis the strength of the magnetic field drops at a linear rate causing us to set the mass selector to a lower current then for the intended mass of the ion. Because this is a bent magnetic, the effect will cause charged particles to focus in the horizontal direction. In addition because the magnetics are beveled, on the top and bottom, there is a focusing in the vertical direction of equal magnitude to the horizontal direction.

2.4. Accelerator Tube

After the H^- ion passes through the mass selector is enters an accelerator tube which will increase the energy of the beam as well as focus it. The tube consists of a series of metal rings separated by glass all connected by resistors in series. The metal rings have a slight tilt to them which will attract any stray electrons. Because the tube is circular in shape the beam is focused in all directions towards the direction of propagation, straight down the center of the tube which we define as the z-axis. This works off the same principals as the Einzel Lens expect it is a series of lens' instead of one. Based upon a gradual increase in potential differences between plates the beam is accelerated down the tube and becomes gradually focused each step of the way. This tube is necessary for the following reason: if the beam enters the Tandem Van de Graaff with an energy of a couple keV it will be focused too quickly.

2.5. Electrostatic Quadrapole Triplet

After the accelerator tube are three sets of four electrodes of alternating charge. From one quadruple to the next (along the direction of propagation) the charges alternate, so nowhere is

there a positively charged electrode adjacent to another positively charged electrode. This set acts to focus the beam in both the horizontal and vertical directions. If we choose to say that the first quadrapole the beam (traveling along the z-axis) sees has the two positive electrodes along the y-axis and the two negative electrodes along the x-axis. The positive electrodes will focus the beam in the y-axis while the negative electrodes will defocus the beam in the x-axis. The next quadrapole has the same orientation but rotated 90 degrees so the beam is focused and spread in the opposite direction as before. We add a third quadrapole to correct for an astigmatism made from the two previous electrostatic quadrapoles.

2.6.   Faraday Cup

A low energy (LE) Faraday Cup is located just after the Electrostatic Quadrapole Triplet and just before the Tandem Van de Graaff. There is also a high energy (HE) Faraday Cup after the Tandem Van de Graaff. It serves as a way to measure the position and focus of the beam. Simply put if the beam is well focused more ions will hit the Faraday Cup resulting in a larger response signal. When the H^- beam collides with the Faraday Cup secondary electrons are produced. A potential wall of -300V is put at the opening of the Faraday Cup so that no negative charges leave this detector, which reduces the error in our signal. At the point of injection, into the Tandem Van de Graaff, the ions have an energy of $E_{inj} = 185$ keV.

2.7.   Tandem Van de Graaff

The accelerator we use here was the eighth King Tandem built by the High Voltage Engineering Corporation [1]. The tank consists of an accelerator tube which is of the same make as described above. Additionally, the tank is filed with SF^6 for its high dielectric strength and high recombination rate. Inside the accelerator tube is a series of two 200 circularly planes, before (Low Energy, LE), and after the terminal, ('High Energy' HE), held together by glass which are under compression, distributed well throughout all planes mechanically, created by a large spring. All the planes are connected by 800 MΩ resistors making a total resistance in the system to be 80 GΩ. At the center of the tank we define the terminal to be the point of maximum potential.

The voltage in the Tandem Van de Graaff is supplied by the mechanical transport of charge. On the HE half of the tank, post-terminal, the charge is supplied by a Laddertron [1] which is a 12 meter long chain of aluminum, stainless steel and plastic [1]. The Laddertron turns at a rate of 12

m/s about two conductive pulleys at either end of the HE half of the tank. Charge is induced on each link of the Laddertron by a high voltage supply, the inductor, of -50kV where the conductive pulley is connected to ground. The Laddertron, with $I_{Laddertron} = 60\mu A$, then carries positive charges from the inductor towards the terminal where the suppressor voltage supply attracts all the positive charge. Thus, the conductive pulley shares its potential with the whole terminal. This potential can be solved using Ohm's Law and is found to be $V_{terminal} = IR = 40\mu A \cdot 80 G\Omega \approx 3MV$. Note that 20 μA are drawn from the terminal to the corona needle which is described below. The efficiency of the Tandem is that the voltage is used twice to accelerate the ions.

At injection we have H^- ions that accelerate towards the terminal. In the terminal the ions hit a carbon foil of density 5 $\mu g/cm^2$, which strips electrons from the beam creating a beam of H^+ ions. At this point the positively charged ions are now accelerated away from the terminal at the same potential that had just prior, attracted it to the terminal.

It is important to have voltage control. This is done by adding a corona needle which sits above the terminal and can be raised or lower depending on how much current one wishes to draw. It also serves to prevent arcing in the tank. For more precise control the corona needle has a feedback loop controlled by a signal measured on a Generating Volt Meter (GVM). In addition to the GVM a Slit Regulation (which I will mention later), located after the Analyzer, will send a feedback signal to the corona needle so that the beam makes a near perfect 90 degree bend at the Analyzer which is based off the energy of the beam.

The final energy of the ions leaving the Tandem is given by

$$E_{tandem} = V_{term} \cdot (1 + q_{ion}) + E_{inj} = 2V_{term} + E_{inj} \approx 6MeV \tag{1}$$

2.8. Magnetic Quadrapole Doublet

After the Tandem is a Faraday cup to record the position of the HE beam, used to further align the beam. If this Faraday Cup is not impeding the propagation of the HE beam then proton beam passes through a Magnetic Quadrapole Doublet. Analogous to the Electrostatic Quadrapole Triplet, we have two sets (doublet) of four magnetic poles (quadrapole), with adjacent poles being opposite, north next to south in all directions. This acts to focus the beam in both the x and y axis. It should be noted that this doublet will cause an astigmatism in the beam. This will be corrected by another Magnetic Quadrapole Doublet later down the line, before the target, that creates an astigmatism in the opposite direction, so both these effects cancel each other.

2.9.   Beam Steerer

The next piece of equipment is another device used to align the beam. The Steerer consists of two pairs of tightly wound coils that are located on each side of the vacuum tube as well as on the top and bottom. These pairs of coils are powered by two bipolar power supplies. A magnetic force is applied in both the x and y direction proportional to the current applied through the coils.

2.10.   Bonner Ball

Because of a malfunction in the Analyzer, the following equipment will not be used to make our ^{11}C nor detect our beam. Instead, we use a Bonner Ball which is a fast neutron detector. It was originally installed to measure radiation levels. The Bonner Ball has spherical neutron counter (LiF) in the center of a polyurethane layer. The reading was viewed via a CCD camera connected to a monitor located in the control room since it is not apart of the typical controls used in this procedure.

2.11.   The Analyzer

To turn the ion beam 90° (so it travels in the initial direction it propagated before the Mass Selector) we use an Analyzer which works much in the same method as the Mass Selector. The primary use of this device is to separate the energies and charges coming from the Tandem Van de Graaff such that it allows the proton beam to be deflected 90° and pass through unimpeded. Particles of energy and charge we are no interested in will collide with the walls. Immediately after the Analyzer is a slit regulation set up where the slits cut off the tail end of our beam, which we approximate to be of Gaussian shape. If the beam has too much or too little energy the Analyzer will deflect the beam off the paraxial axis then these slits will detect more energy in the form of a current then wanted. The detected signal in terms of the current is sent to the feedback in the Corona Needle which will either increase or decrease the current drawn from the terminal. This correction will change the energy of the beam so that it leaves the Analyzer on axis, resulting in a reduced response on the slit regulator. After the slit regulator is another Faraday Cup which we will call the Image 2 Faraday Cup to give further measurements of the beam alignment.

We now enter the detection room which has several more focusing optics as well as where our Boron target will be placed. Once these are explained we will have full knowledge of how we make our ion beam, how the Tandem Van de Graaff works, and how we align the beam to target.

2.12.   Switcher Magnet

Before the Switcher, is a Magnetic Quadrapole Triplet used to focus the ion beam is both directions. It is apparent that once the beam is focused, it must be refocused after some time of flight. This is the reason we have all these electro- or magneto-optical components along our beam line. The Switcher is essentially a giant magnetic, whose magnitude is controlled by an applied current,that has a vacuum tube inside. It has 7 different exit ports that have been used for various experiments. For this experiment we are going to use the 30° port. After the Switcher is another Magnetic Quadrapole Doublet that will focus our beam and also correct for the astigmatism created by the first Magnetic Quadrapole Doublet. Then the beam passes through another Steerer used as the last device to align the beam to target. The target is behind this Steerer and is placed in a frame. With no sample in the target frame, the beam passes through and is incident on the beam dump. The beam dump is lead lined stainless steel and will be used to align the beam as discussed below. The beam dump and target plate are connected to electronics to measure their signals which is used in aligning the beam.

3.   TUNING THE BEAM

Now that we have a clear understanding of all the devices involved in making the ion source, accelerating and creating a positive ion beam we can discuss the procedure to align the beam to target. The procedure that will be done is to align a beam of Oxygen, AU = 16, because there is always Oxygen present in the system, and then change the variables in the mass selector to allow Hydrogen to pass. Due to a current repair of the Analyzer taking place we place the Boron target just before the Bonner Ball and maximize our signal on the Bonner Ball to indicate a well aligned proton beam.

The first step is to turn on all the components involved in the Ion Source and to set the extraction voltage to an initial setting of 14.96 kV. Digital controls are used via satellite computers connected to LabView to set the values in each various component. The ionizer has a voltage set to V = 8.49 V and current I = -4.10 A such that its temperature will ionize the Cs then we set the Mass Selector to optimize the passage of Oxygen ion. The Cathode potential attracting the Cs ions was set to 3.94V with a current of 0.56 A. We soon moved onto changing the mass selector so that it allowed protons to pass, mass = 1 AU. Once this is done the applied voltage to the Einzel Lens was set to 4.46 kV. After the proton beam passes through the Mass Selector we set the voltage on

the Electrostatic Quadrapole Triplet to X: [1.58 kV, 1.58kV], Y: [1.86 kV, 1.72 kV] to maximize the current reading on the LE Faraday cup. At this point the LE Faraday Cup had a reading of 66.24 nA. This is all shown below.
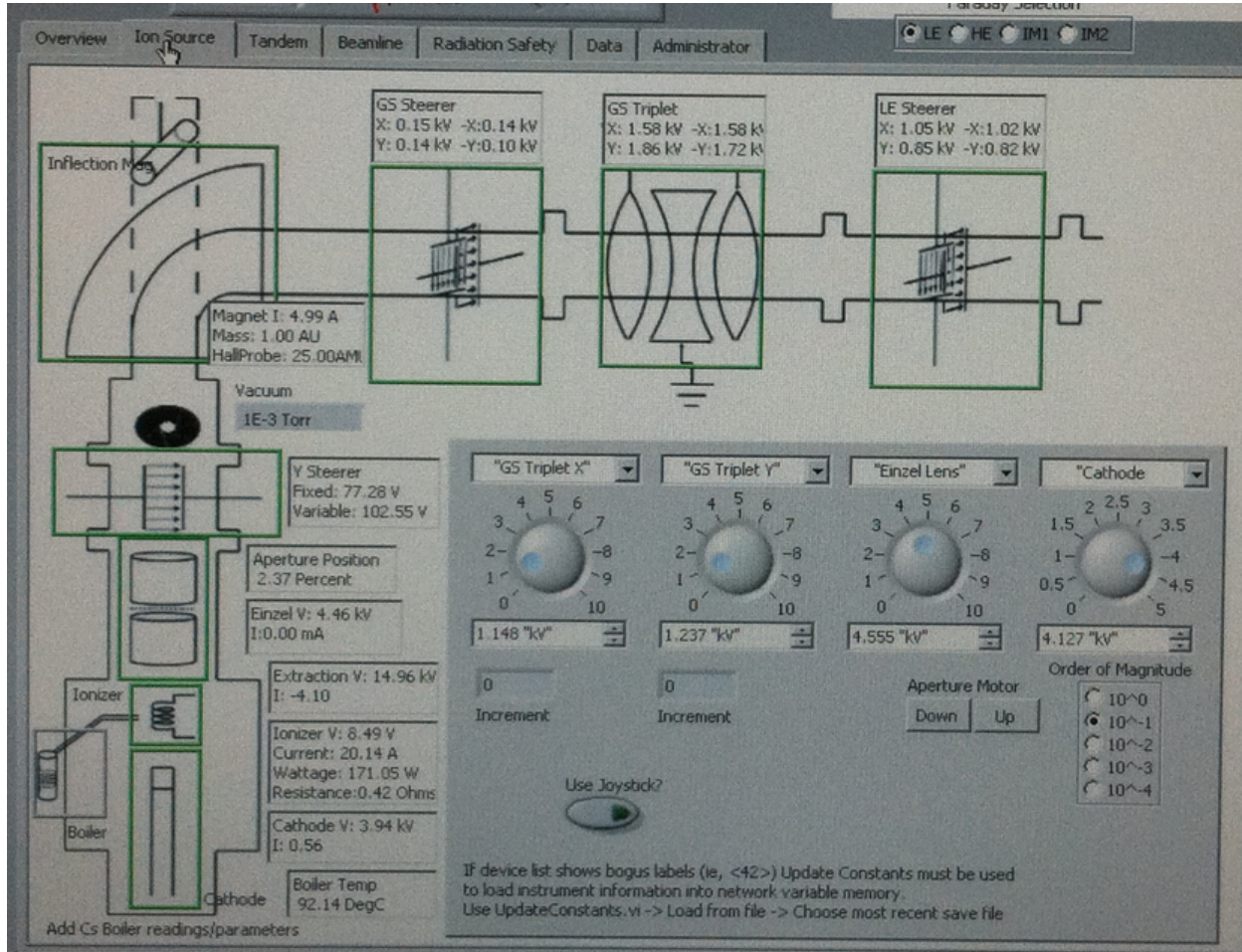

FIG. 1: This is a picture of the LabView program took on the day ^{11}C was made. Both a diagram of the Ion Source and LE optics with as their corresponding voltage and current settings are shown.

When the LE Faraday Cup has its signal maximized we move onto the the settings for the components Tandem Van de Graaff which have been listed in Section [2.7]. A second run of making subtle changes to equipment on the LE side were done to maximize the signal on the HE Faraday cup. The largest change made to maximize the HE Faraday cup's reading was the LE steerer which we set to X: [1.22 kV, 1.18 kV], Y: [0.93 kV, 0.90 kV] and is shown in the figure below. We maximized the HE Faraday's cup reading to 51.8 nA to indicate the beam was well aligned coming out of the Tandem. The next step was to remove the HE Faraday cup (which impedes the beam propagation) and then maximize the Bonner Ball's reading as our final detection to indicate

the alignment of the beam.

As stated, the beam then passes though a Magnetc Quadrapole Doublet (MQD) and the HE Steerer before being incident on the Bonner Ball. These two devices act as our final optical components to align the beam to target. We were able to maximize the reading on the Bonner Ball to 14mRem/hour with an average reading of 7 mRem/hour as we were changing the settings to the MQD and HE Steerer. These final settings are shown below.
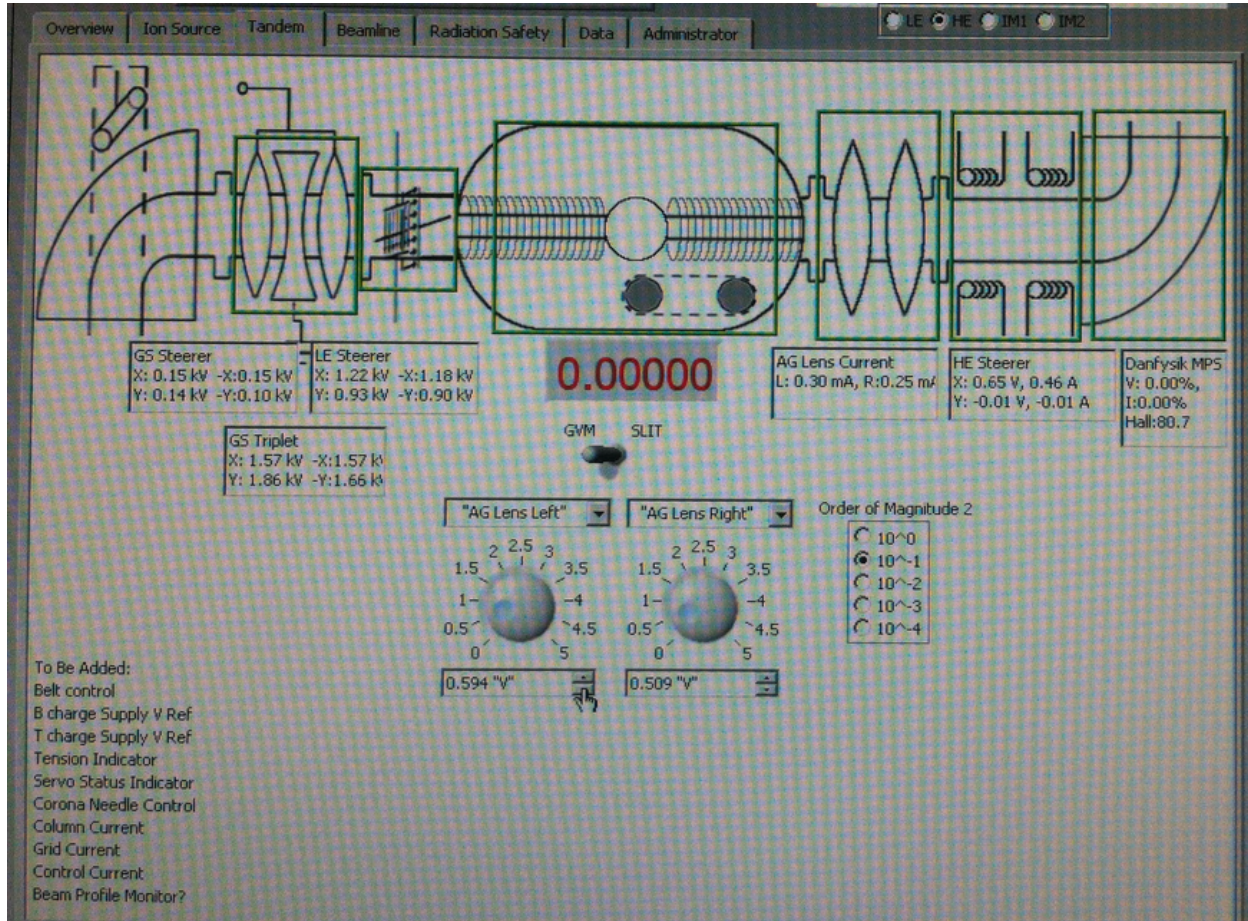

FIG. 2: This is a picture of the LabView showing the optics both before and after the Tandem which is at the center of this picture. Both the MQD (AG Lens here) and HE steerer settings were set to maximize the reading on the Bonner Ball.

We then kept the beam hitting the Boron target for approx. 15 minutes to make a 'hot' sample. Once Rich Lefferts assured us we made plenty of ^{11}C we went into the Tandem room and he safely removed the Boron target and brought it back to the detection room because he is properly trained to handle such radioactive material. To ensure safety my partner and I remained behind the 2 mRem/hour distance of exposure which we found to be roughly half a meter for our given sample.

4. DATA AND ANALYSIS

4.1. Calibration of Equipment

Using a sodium sample ^{22}Na, whose has a lifetime of over two years, we can calibrate the detection equipment. This is done because the decay of ^{22}Na emits positrons which result in pair annihilation whose resultant is a pair of gamma rays traveling in opposite directions. This is analogous to the decay of ^{11}C. This is because the gamma rays emitted have energy of about 511 keV, so we calibrate our system to detect said gamma rays using our ^{22}Na sample. It must be noted that the ^{22}Na decay results in the production of two gamma ray pairs with energies: .511 MeV and 1.274 MeV [2]. The higher energy gamma rays results from electron capture, while the lower energy gamma rays (0.511 MeV) correspond to the pair annihilation we are interested in. The nuclear reaction we use to make ^{11}C is:

$$^{11}B + p \rightarrow {}^{11}C + n \tag{2}$$

Here the ^{11}C will decay 100% of the time through positron emission via:

$$^{11}C \rightarrow {}^{11}B + e^+ + \nu_e \tag{3}$$

Once the positrons have similar momentum to local electrons they will annihilate resulting in two gamma rays being produced at nearly 180° apart due to the rest mast of the electron being much greater than the momentum of the electron. This reaction is shown below.

$$e^+ + e^- \rightarrow \gamma\gamma \tag{4}$$

where $e^{+,-}$ corresponds to a positron and electron.

The figure below shows a diagram of our coincidence (two gamma rays, produce by pair annihilation, measured at the same time) detection system.
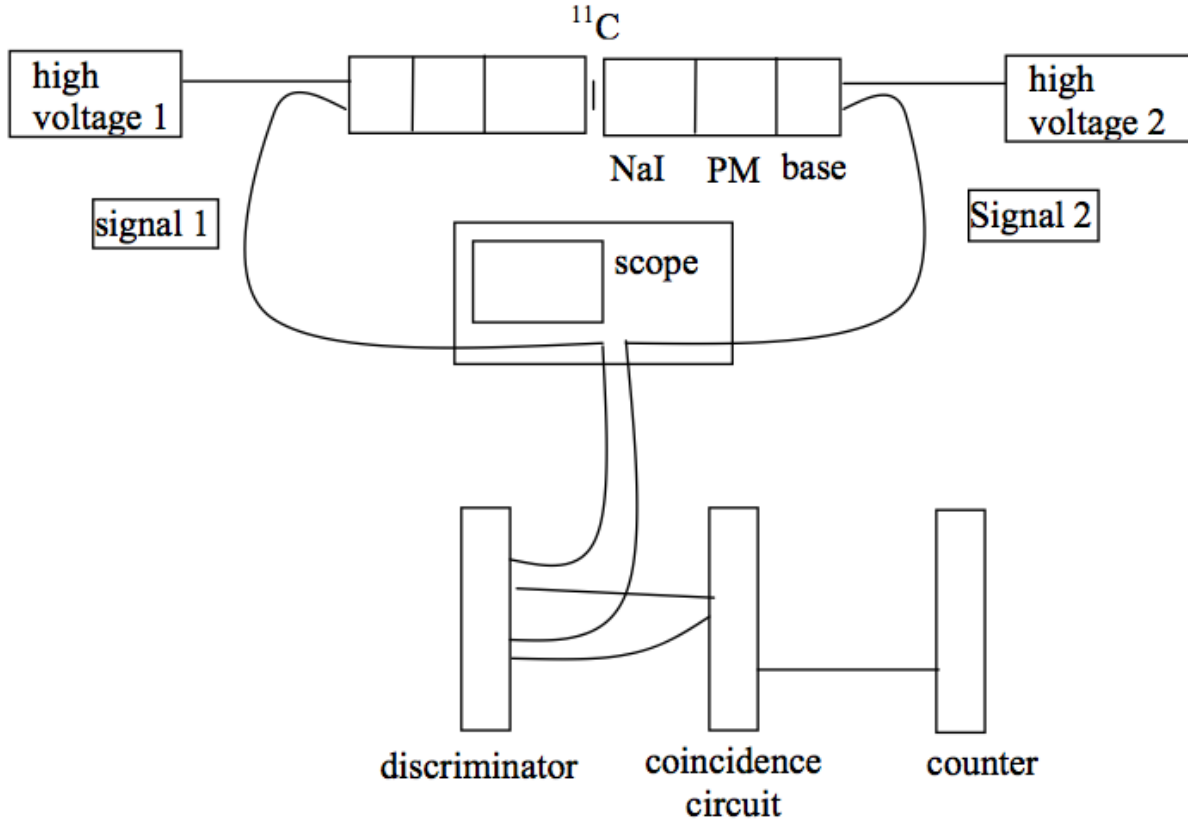
FIG. 3: A schematic depicting the equipment used to detect coincidences. After the discriminator we delay signal 2 29 ns for reasons discussed below.

To detect both gamma rays (a coincidence) we use two Bicron NaL(TI) 2" crystals each connected to a photomultiplier tube (PMT). These two are enclosed in a sealed metal casing. Two Oretec 0-2 kV bias supplies at a negative high voltage are used to power the PMT. Because the two are not perfectly identical we drive them at different voltages to produce signals of the same amplitude. We choose to supply the left detector, Detector 1,with a voltage of -1.34 kV and the right detector, detector 2, at -1.23 kV. This choice resulted in signals corresponding to the .511 MeV gamma rays of 55 ± 2 mV measured on a Tektronix TDS 2024B oscilloscope. The NaI crystal and PMT detect gamma rays through the following procedure. A gamma ray enters the NaI crystal and looses energy via the Compton effect, this is why we see a distribution of peaks on the oscilloscope. The light that is directed towards the cathode of the PMT has enough energy to strip electrons from the cathode via the photoelectric effect. These free electrons are accelerated, based upon an applied potential, towards a dynode. Upon impact the electron removes more electrons which are then accelerated to a second dynode. The process repeats as the electrons are directed

towards the anode at the opposite end upon which an electrical signal is produced. The signal gain from this process is a ratio of the number of electrons reaching the anode to the initial number of free electrons at the cathode which is based upon the voltage drop across the dynodes. This allows us to distinguish between the two gamma rays of different energies. In other words, the higher energy gamma rays will result in a stronger signal as they have more energy to free electrons so we can differentiate between the gamma rays we want to detect and those that have no insight to this experiment.

The electrical signal from the anode then passes though a discriminator which removes any negative voltages to low to be considered indicators of a coincidence at 0.511 MeV. This is manually set by the threshold for each input. The discriminator also acts to turn the analog signal to a logic signal so that the logic gate can read it. To find the optimal value we measured the coincidence count as a function of the threshold voltage for signals at 55 mV. This is shown below.
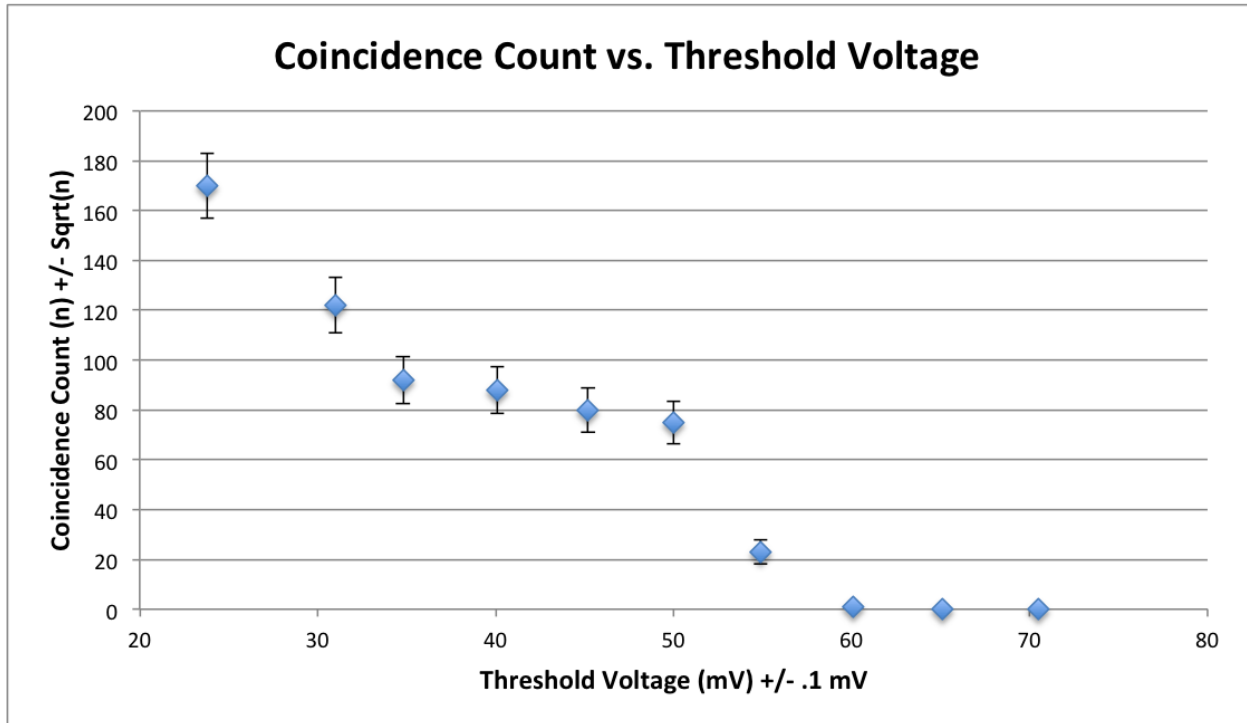

FIG. 4: Each point indicates the average coincidence count for three runs each of 2ns of length for a given threshold voltage. We found the coincidence count is reduced significantly if the threshold voltage is set to the peak amplitude of -55 mV and decreases to 0 for larger values of threshold voltage as expected.

We see that when our threshold is low we count many more events. While these are probably real coincidences we choose to set the threshold voltage at 50.0 mV so we reduce background and have better path geometry for the gamma ray to be detected. The pulse length is triggered to the

rising edge of the signal from the detector, and is sent into the logic gate. In order to minimize the rate of accidentals given by

$$A \approx \sigma N_1 N_2 \qquad (5)$$

the logic pulses need to small in width. In conjunction, the pulses need to be large enough that the error in the rising edge (20 -25 ns) will not prevent the logic gate from measuring an event. Below we measured the coincidence count as a function of the pulse width (same for both detectors) for 2 ns runs with the threshold set at 50 mV and signals at 55 mV. For all these measurements the error in each count, n, was taken to be $\sqrt{n}$.
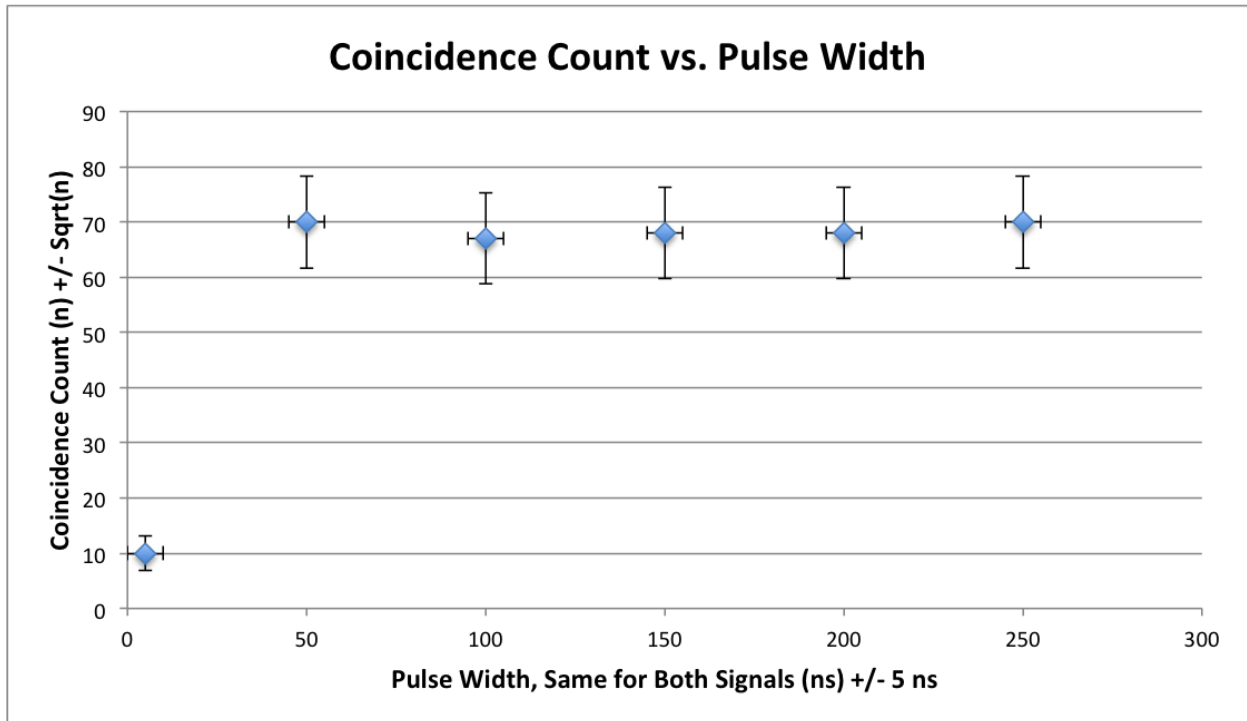

FIG. 5: Each point indicates the coincidence count for a given pulse width, which is the same for each detector.

We find that for a wide range of pulse widths the coincidence count remains the same. As a result we chose to maintain each pulse's width to be 50 ± 5 ns. In addition, it is important to measure the coincidence rate as a function of the delay between pulses before entering the logic gate. These results are shown below.
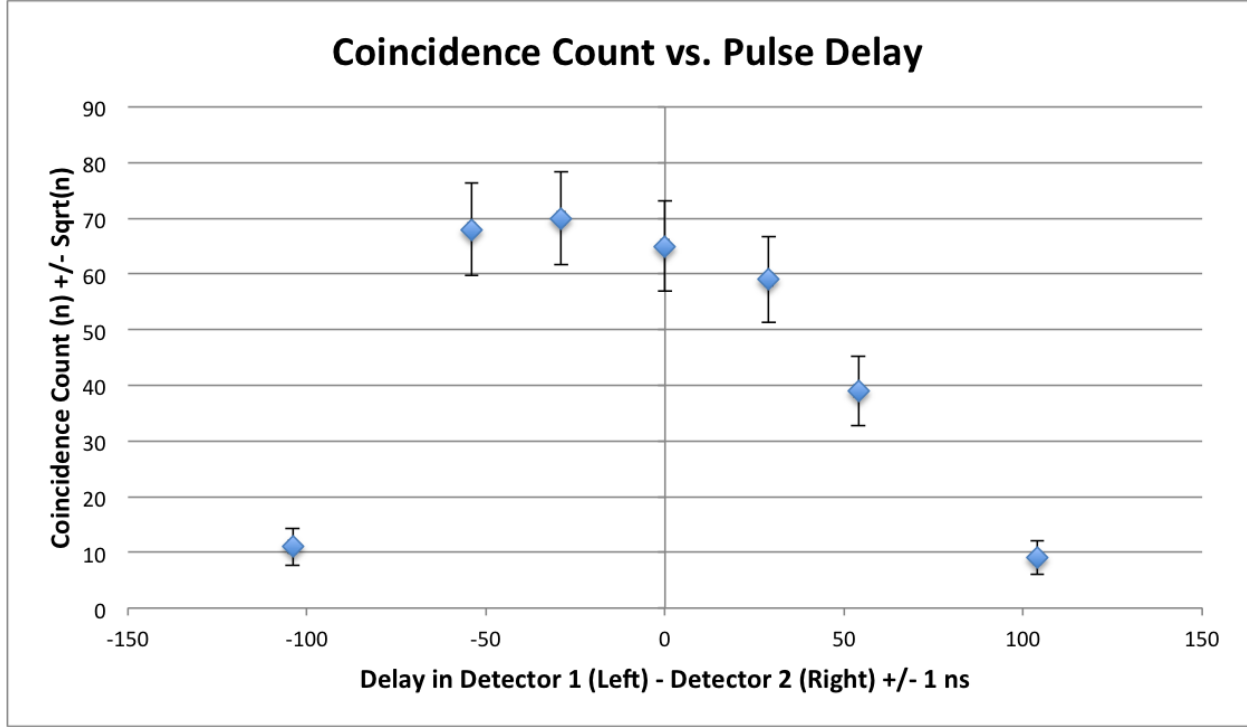
FIG. 6: We find that the coincidence count is strongly dependent on the delay between the pulses. The plateau at the top (-50 ns → 0 ns) is consistent with Reference [3] and indicates the resolving time as a well as what each pulse's width should be.

Based upon these measurements we choose to set the delay between the pulses at -29 ± 1 ns because it is at the center of that plateau. At this point we are readily equipped to measure the coincidence count of a given sample. We can also find an accurate measurement of the rate of accidentals, which are systematic errors and should be subtracted from a given count to give an accurate measurement. This is done using the relation given in Reference [2] and is shown below

$$A = Accidentals_{per200s} = \sigma \frac{N_1}{200s} \frac{N_2}{200s} \cdot 200s \qquad (6)$$

where N_1 is the singles count from Detector 1, N_2 is the singles count from Detector 2, and σ is the resolving time of our detection system and was found to be $50 \pm 5ns$. Using these values we found that $A = 912.962 \pm 91.3011$ counts per 200 s. We will compare this value later to our fit.

The table below is a summary of the chosen detection parameters to measure gamma ray coincidences. Note that the threshold setting is changed from 50 mV to 45 mV because other groups were measuring many less counts then expected because their threshold was too close to their peak height. While this did not not seem to affect our measurements using ^{22}Na, we still

lowered it to ensure we would not limit the amount of counts when detecting gamma rays from ^{11}C.

HV to Detector 1 (Left)	-1.34 kV Makes a 55 $\pm$ 2 mV Signal
HV to Detector 2 (Right)	-1.23 kV Makes a 55 $\pm$ 2 mV Signal
Threshold Setting	45 $\pm$ .1 mV (Both Detectors)
Time Delay Between Detectors	-29 $\pm$ 1 ns (Detector 1 - Detector 2)
Pulse Width	50 $\pm$ 5 ns (Both Detectors)

Using these parameters we now measure the coincidence count rate for 1 μCi ^{22}Na source.
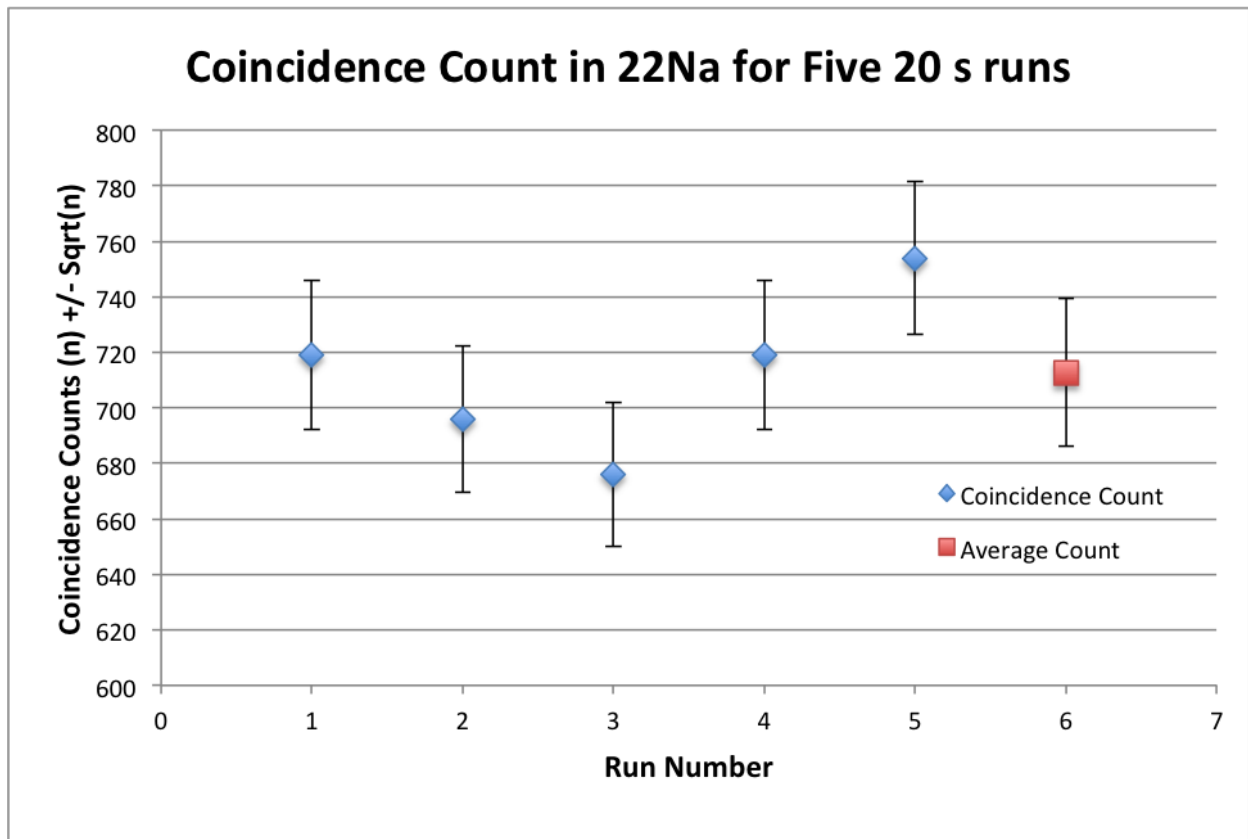

FIG. 7: The average count of these five runs is 712.8 $\pm$ 26.69 with a standard deviation of 26.11, which was found using Eq.(1.8) from Reference [4].

These results are consistent with the data from the above graphs for the reason that in those 2 s intervals we measured approx. 70 counts thus for a 20 s run we should see approx. 700 counts which is what is shown above. While the there is a 80 count spread between the maximum count measured here (719) and the minimum (676) we find that each other measurement is within the range of the other measurements when one takes into account the error. We do not believe this

deviation will hinder our final calculation for the lifetime of ^{11}C because the number of counts will decay exponentially while the emission of gamma rays from ^{22}Na is near constant but clearly fluctuates. In addition, any ambient radioactive sources and having not including the rate of accidentals per second may have added to the error in this measurement.

4.2. Half-Life of ^{11}C

The nuclear decay of any sample can be represented as an exponential decay. After a given time the remaining amount of that sample is given as

$$N(t) = N_0 e^{-\lambda t} = N_0 e^{\frac{-ln(2)t}{t_{1/2}}} \tag{7}$$

where N_0 is the initial amount of the sample, t is the time elapsed, $\lambda = \frac{ln(2)}{t_{1/2}}$, and $t_{1/2}$ is the half-life of the sample. Because the exact remaining amount, and the initial amount could not be measured in this experiment we count the number of coincidences over a time period of 200s and then repeat after recording these values. It is also necessary to include accidentals which are due to the logic gate and the constant rate of background radiation being detected. The new relation we use is given below

$$N(t) = N_0 e^{-\lambda t} + N_0' e^{-\lambda' t} + C \tag{8}$$

where N_0' is the initial number amount of accidentals, λ' is the half-life of accidentals, and C is the time average background coincidence rate which we measured to be 2 counts per 200s.

Using the Solver package in Excel, the parameters of $N_0, \lambda, N_0', \lambda'$ were varied in order to get the reduced χ^2 closets to 1. The formulas for χ^2 and reduced χ^2 are shown below and can be found in References [4],[5].

$$\chi^2 = \sum_N \frac{(N_{measured} - N_{estimated})^2}{\sigma^2} \tag{9}$$

$$\text{Reduced}\chi^2 = \frac{\chi^2}{N - d} \tag{10}$$

Here, N is the number of data points, $\sigma = \sqrt{counts}$ and d is the number of constraints. The result of using the Solver Package is shown below.
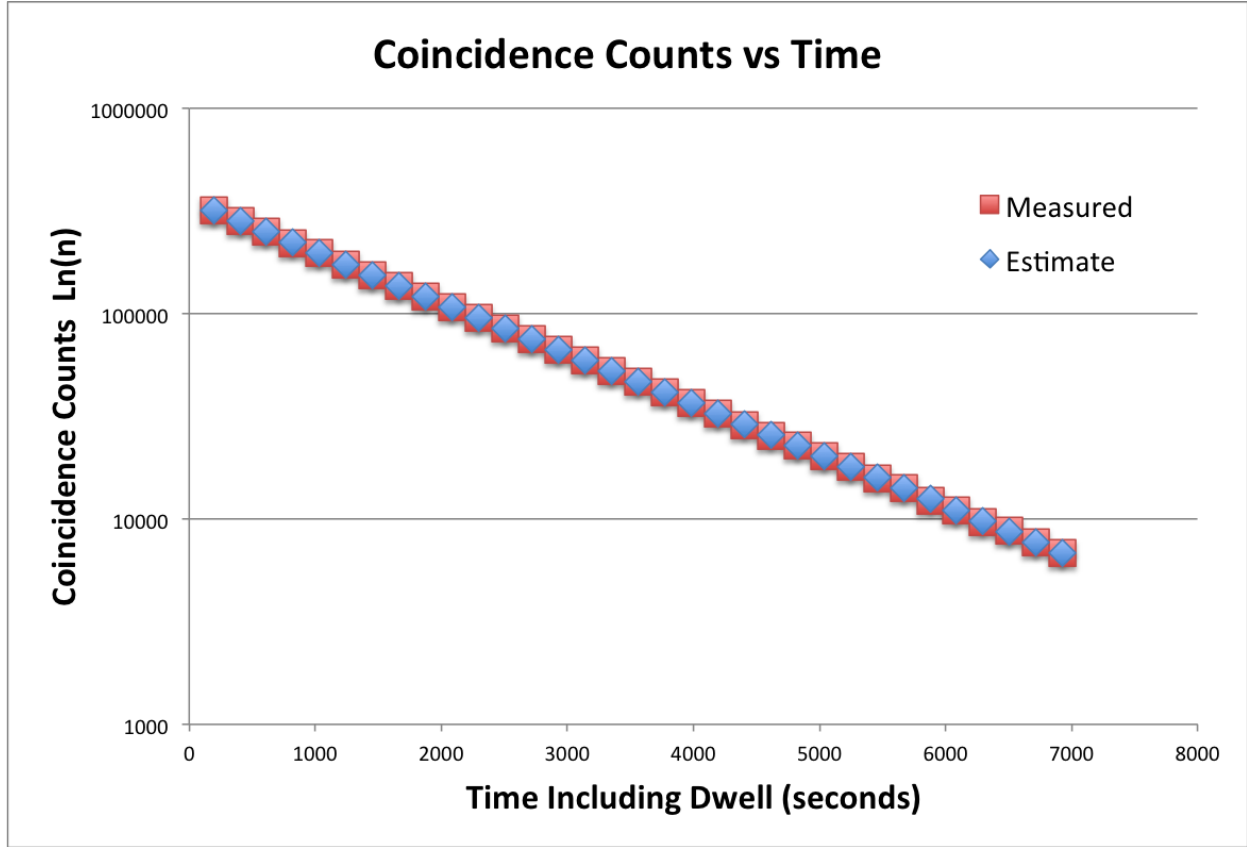
FIG. 8: The number of counts vs time for both our measured and expected values are shown. The expected values were found using the Solver package in Excel. We see that these match up very well, so much so it is hard to differentiate between the two. In addition, because the y-axis is plotted on a log scale, the error bars were smaller than the markers so they can not be seen.

Using the Solver package the following values were found.

N_0	$2{,}927{,}906.09 \pm 1711.11$ counts
λ	$5.6868 \cdot 10^{-4} \frac{1}{s}$
$t_{1/2}$	20.310 minutes
N_0'	9275.60 ± 96.3099 counts
λ'	$3.089 \cdot 10^{-3} \frac{1}{s}$
$t_{1/2}'$	3.738 minutes

While this measurement for the number of accidentals is an order of magnitude greater than what we calculated prior I am more prone to trust this result because of the accurate value found for the half-life of the sample. To find the uncertainty in our measurement of λ, χ^2 was plotted for various values of λ because the standard deviation for a variable found by using Solver is equal to the difference of these values when $\chi_{new}^2 = \chi^2 + 1$. The result is the parabolic curve shown below.
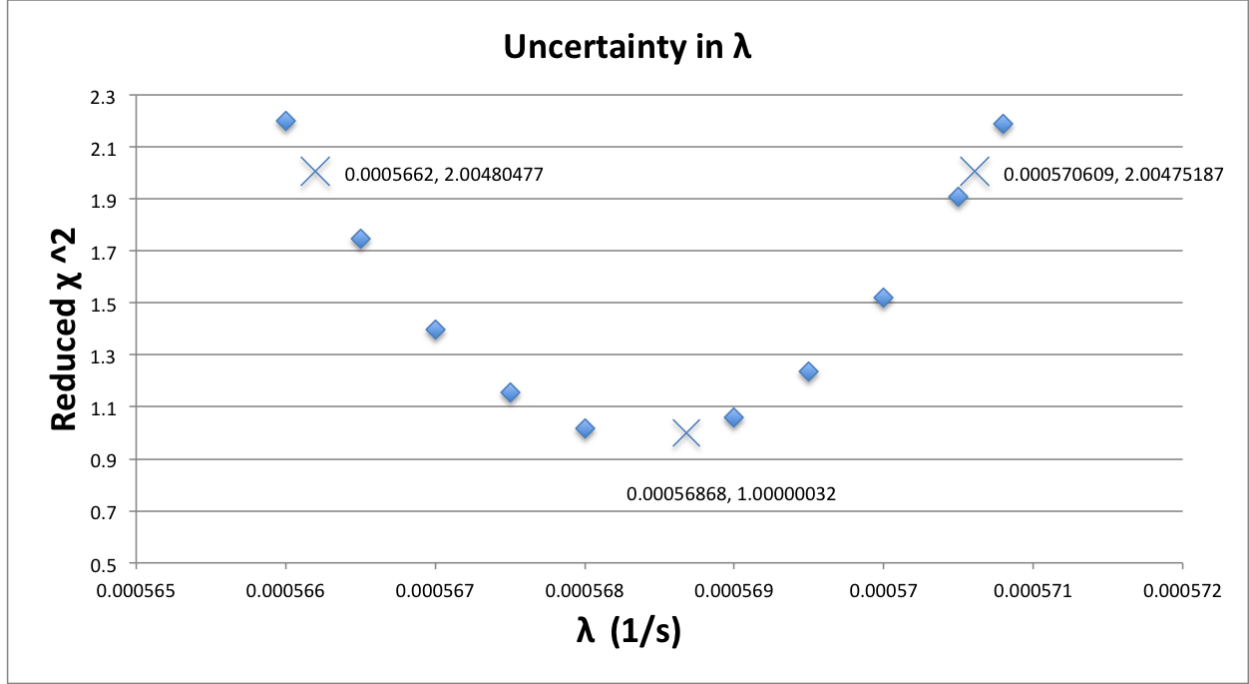
FIG. 9: This graph shows the parabolic nature of χ^2 as a function of λ. We use this to find the uncertainty of λ.

Using the information shown above we find that $\lambda = 5.6868^{+0.00191}_{-0.00218} \cdot 10^{-4} s^{-1}$ which corresponds to $t_{1/2} = 20.31^{+0.089}_{-0.068}$ min. This is in agreement with the accepted value for the half-life of ^{11}C which is $20.334(24)$ min [6]. Our measured value is well within one standard deviation and has a percent error of 0.1%

5. CONCLUSION

It has been shown that using a Tandem Van de Graaff we can accelerate protons to an energy of approx. 6 MeV. In doing so we created a ^{11}C sample by bombarding ^{11}B with these high energy protons. We measured a half-life of $t_{1/2} = 20.31^{+0.089}_{-0.068}$ min which is very near the accepted value of $20.334(24)$ min. Sources of error may have come from minor errors in our detection system and the Solver package used to fit to the measured values.

6. ACKNOWLEDGEMENTS

I would like to greatly thank Rich. Lefferts for his patience and expertise in explaining the experimental setup, detection system, and for handling the ^{11} sample.

7.   REFERENCES

1. PHY 445. **Van de Graaff: Carbon-11 Lifetime Writeup**. 2013

2. Richard B. Firestone. **Table of Isotopes: Eighth Edition**. *John Wiley & Sons Inc.* 1996

3. W. R. Leo. **Techniques for Nuclear and Particle Phyiscs Experiments: A How-to-Approach, Second Edition**. *Springer - Verlog.* 1994.

4. Philip R. Bevington, D. Keith Robinson. **Data Reduction and Error Analysis for the Physical Sciences: Third Edition**. *McGraw-Hill.* 2002.

5. John R. Taylor. **An Introduction to Error Analysis: The Study of Uncertainties in Physical Measurements Second Edition**. *University Science Books.* 1997.

6.   **National Nuclear Data Center, Brookhaven National Laboratory, Chart of Nuclides**. *http://www.nndc.bnl.gov/chart/reCenter.jsp?z=6n=5.*